$(d, {}^3\mathrm{He})$ reactions for the formation of deeply bound pionic atoms

S. Hirenzaki,[(1)] H. Toki,[(1,2)] and T. Yamazaki[(3)]
[(1)]RIKEN, 2-1 Hirosawa, Wako, Saitama 351-01, Japan
[(2)]Department of Physics, Tokyo Metropolitan University, Hachiohji, Tokyo 192, Japan
[(3)]Institute for Nuclear Study, University of Tokyo, Tanashi, Tokyo 188, Japan
(Received 21 May 1991)

We have studied theoretically the proton pick-up $(d,{}^3\mathrm{He})$ reactions leading to deeply bound pionic atoms. The forward scattering cross sections for an incident energy $T_d = 600$ MeV have been calculated using the effective number approach for the $^{208}\mathrm{Pb}$ target nucleus. It was found that the pionic $2p$ state has the maximum cross section among all calculated states. We conclude that $(d,{}^3\mathrm{He})$ reactions produce pionic atoms in a detectable manner.

I. INTRODUCTION

We have investigated the $(d,{}^3\mathrm{He})$ reactions in detail for the formation of deeply bound pionic atoms, and found that the $(d,{}^3\mathrm{He})$ reaction is much more favorable than the (n,p) reaction for the search. Deeply bound pionic atoms were investigated by Toki and Yamazaki [1] and were predicted to have narrow widths due to the repulsive pion-nucleus optical potential that pushes the pion wave function outwards [2]. These states cannot be observed in standard pionic-atom experiments that detect pionic x rays. Hence, they proposed the use of pion-transfer reactions such as (n,p) and $(d,{}^2\mathrm{He})$. Following their suggestions, deeply bound pionic states were searched for by using the (n,p) reaction at $T_n = 420$ MeV at TRIUMF [3]. No positive evidence was observed in the experiment. To obtain better statistics with better resolution, another reaction $(d,{}^2\mathrm{He})$ at $T_d = 1000$ MeV at SATURNE [4] was measured and its analysis is in progress. It was pointed out that the charge-exchange pion-transfer reactions at large momentum transfer are sensitively affected by initial- and final-state interactions. It is found that the cross sections are about two orders of magnitudes smaller [3] than the plane-wave Born-approximation predictions of Refs. [1,2]. The same was also reported by Nieves and Oset [5].

The formation of deeply bound pionic atoms by (n,d) reactions was also studied theoretically [6]. It was found that the distortion effects of (n,d) reactions are smaller than that of (n,p) reactions since the angular momentum matching condition is well satisfied in (n,d) reactions. It was concluded that (n,d) reactions are more suitable for pionic-atom detection[6] and an experiment of this reaction at $T_n = 400$ MeV is in progress at TRIUMF [7]. However, the weak neutron beam makes the experiment extremely difficult. We, therefore, have studied the $(d,{}^3\mathrm{He})$ reaction for deeply bound pionic-atom formation which uses a strong deuteron beam.

We show the schematic diagram for $(d,{}^3\mathrm{He})$ reaction in Fig. 1. The Q value of the reaction is given by

$$-Q = \omega + S_n(j_n) - [M_n + M_d - M_3] = m_\pi - B_\pi + S_n(j_n) - 6.787 \text{ MeV} , \quad (1)$$

where ω is the excitation energy of a pionic state with a neutron hole and $S_n(j_n)$ is the separation energy of the neutron from the orbital j_n. The pionic-atom binding energy is given by B_π. For $^{208}\mathrm{Pb}$ target the main contribution comes from the following orbitals: $p_{1/2}$ (ground state, $S_n = 7.367$ MeV), $f_{5/2}$ ($S_n = 7.937$ MeV), $p_{3/2}$ ($S_n = 8.264$ MeV), and $i_{13/2}$ ($S_n = 9.000$ MeV).

We organize this paper as follows. In Sec. II we develop the formulation of $(d,{}^3\mathrm{He})$ reactions leading to deeply bound pionic atoms using the effective number approach. We then present in Sec. III the numerical results of cross sections that include the distortion effects on the incoming and outgoing particles. In Sec. IV we discuss the background and quasifree pion production cross sections. Section V summarizes the present study.

II. EFFECTIVE NUMBER APPROACH

The effective number approach is often used to calculate a reaction cross section by using the cross section of the elementary reaction. This approach is justified from

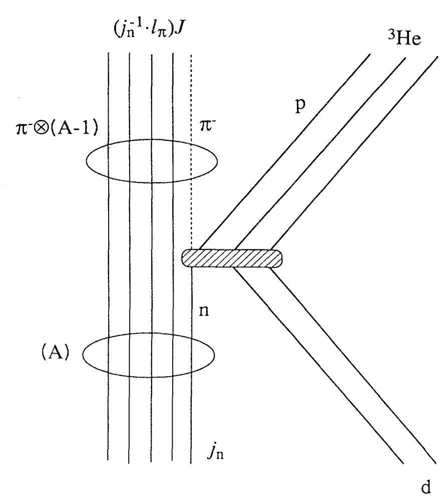

FIG. 1. Diagram for proton-pick-up $(d,{}^3\mathrm{He})$ reactions to form pionic bound states on a neutron-hole state.

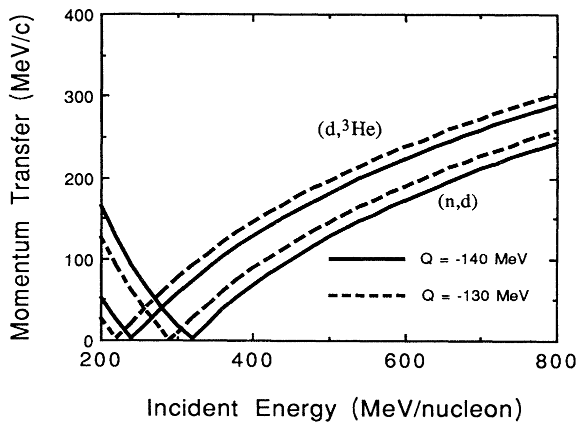

FIG. 2. Momentum transfers in the (n,d) and $(d,^3He)$ reactions on ^{208}Pb for $-Q=130$ and 140 MeV as functions of the incident energy per nucleon.

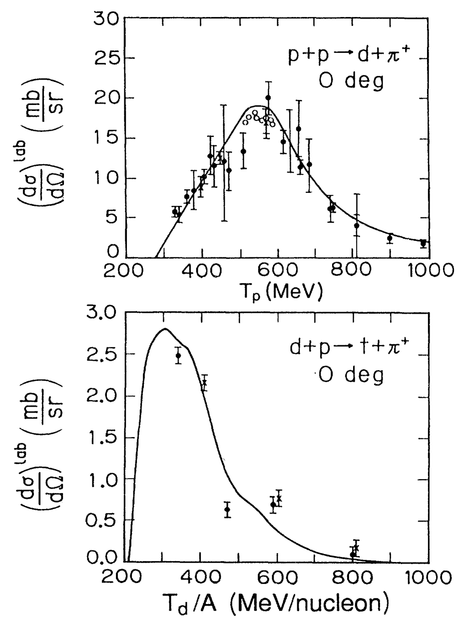

FIG. 3. (a) The differential cross section $(d\sigma/d\Omega)^{\text{lab}}$ at 0° for $p(p,d)\pi^+$ as a function of the incident energy T_p, derived from the experimental values of $(d\sigma/d\Omega)^{\text{c.m.}}$ for $p(p,\pi^+)d$. The zero-degree cross sections are determined from the fitting of the experimental angular distributions at each energy. The cross sections are taken from different sources [11–13]. (b) The differential cross section $(d\sigma/d\Omega)^{\text{lab}}$ at 0° for $p(d,t)\pi^+$ as a function of the incident energy T_d/A(MeV/nucleon), derived from the experimental values for $d(p,\pi^+)t$ [10,14]. The solid curve is obtained by multiplying 1.7 to the theoretical result of Fearing [10] to match the experimental cross sections.

the recoilless kinematics, in which a transferred particle (in this case pion) carries little momentum in the target frame. This condition is fulfilled at around $T_d=600$ MeV (300 MeV/nucleon) as can be seen in Fig. 2, which is the energy we consider in this paper.

The pionic-atom formation cross section can be written in the effective number approach as [9]

$$\left[\frac{d\sigma}{d\Omega}\right]_{dA\to{}^3\text{He}(A-1)\pi} = \left[\frac{d\sigma}{d\Omega}\right]^{\text{lab}}_{dn\to{}^3\text{He}\,\pi} N_{\text{eff}}\ , \tag{2}$$

with

$$N_{\text{eff}}=\frac{1}{2}\sum_{Mm_s}\left|\int \chi_f^*(\mathbf{r})\xi^*_{1/2,m_s}(\sigma)[\phi^*_{l_\pi}(\mathbf{r})\otimes\psi_{j_n}(\mathbf{r},\sigma)]_{JM}\chi_i(\mathbf{r})d^3r\,d\sigma\right|^2 . \tag{3}$$

Here, $(d\sigma/d\Omega)_{dA\to{}^3\text{He}(A-1)\pi}$ indicates the pionic-atom formation cross section for the $d+A\to{}^3\text{He}+[(A-1)+\pi^-]$ reaction and $(d\sigma/d\Omega)_{dn\to{}^3\text{He}\,\pi}$ denotes the elementary differential cross section at forward angles for $d+n\to{}^3\text{He}+\pi^-$ in the laboratory system, which is related to the c.m. cross section by

$$\left[\frac{d\sigma}{d\Omega}\right]^{\text{lab}} = \left[\frac{p_h^{\text{lab}}}{p_h^{\text{c.m.}}}\right]^2\left[\frac{d\sigma}{d\Omega}\right]^{\text{c.m.}}\ , \tag{4}$$

where p_h^{lab} and $p_h^{\text{c.m.}}$ are the laboratory and the center-of-mass momenta of the outgoing ^{3}He, respectively.

We use the experimental data of $d+p\to t+\pi^+$ as the elementary cross section, $d+n\to{}^3\text{H}+\pi^-$, by assuming charge symmetry. The experimental zero-degree cross sections for $p(d,t)\pi^+$ in the laboratory frame are shown in Fig. 3 at various energies together with the $p(p,d)\pi^+$ cross sections [6]. The (d,t) cross section is an order of magnitude smaller than that of (p,d). The behavior of the cross section was well understood in terms of the form factor for capturing a deuteron in triton [10]. The solid curves in the figures are the fitted theoretical curves. Since the (d,t) cross section has the largest value at $T_d=600$ MeV (300 MeV/nucleon), we investigate $(d,^3\text{He})$ reaction at this energy in this paper.

The effective number N_{eff} contains the pionic-atom $\phi_{l_\pi}(\mathbf{r})$ and neutron-hole $\Psi_{j_n}(\mathbf{r},\sigma)$ wave functions with a resultant angular momentum J. The spin wave function $\xi_{1/2,m_s}(\sigma)$ with averaging over m_s is introduced so as to take into account the possible spin directions of the neutrons in the target nucleus. χ_i and χ_f denote the initial and final distorted waves of the projectile and the ejectile, respectively.

We use the eikonal approximation, in which the distorted waves are approximated as plane waves with a distortion factor $D(\mathbf{b})$, as

$$\chi_f^*(\mathbf{r})\chi_i(\mathbf{r})=\exp(i\mathbf{q}\cdot\mathbf{r})D(\mathbf{b}) \tag{5}$$

with

$$D(\mathbf{b})=\exp\left[-\frac{1}{2}\int_{-\infty}^{\infty}\bar{\sigma}\rho(\mathbf{b},z')dz'\right]\ , \tag{6}$$

TABLE I. The effective numbers $N_{\rm eff}$, for the ^{208}Pb$(d,{}^3$He) reaction at $T_d=600$ MeV leading to various pionic states $[(nl)_\pi j_n^{-1}]J$ with $j_n=p_{1/2}$ $S_n=7.367$ MeV. SUM denotes the summed value for each J multiplet with the same pionic and neutron-hole configuration.

l_π	J	$[j_n=p_{1/2}]$					
		1s	2s	3s	4s	5s	6s
0	$\frac{1}{2}$	1.05×10^{-3}	2.04×10^{-4}	7.46×10^{-5}	3.65×10^{-5}	2.03×10^{-5}	1.24×10^{-5}
		2p	3p	4p	5p	6p	
1	$\frac{3}{2}$	2.12×10^{-3}	5.85×10^{-4}	2.47×10^{-4}	1.26×10^{-4}	7.30×10^{-5}	
	$\frac{1}{2}$	5.25×10^{-3}	1.48×10^{-3}	6.29×10^{-4}	3.22×10^{-4}	1.87×10^{-4}	
	SUM	7.37×10^{-3}	2.06×10^{-3}	8.76×10^{-4}	4.49×10^{-4}	2.59×10^{-4}	
		3d	4d	5d	6d		
2	$\frac{5}{2}$	4.13×10^{-4}	2.12×10^{-4}	1.15×10^{-4}	6.76×10^{-5}		
	$\frac{3}{2}$	3.19×10^{-4}	1.63×10^{-4}	8.84×10^{-5}	5.17×10^{-5}		
	SUM	7.32×10^{-4}	3.75×10^{-4}	2.04×10^{-4}	1.19×10^{-4}		
		4f	5f	6f			
3	$\frac{7}{2}$	4.32×10^{-6}	3.59×10^{-6}	2.58×10^{-6}			
	$\frac{5}{2}$	1.16×10^{-5}	9.68×10^{-6}	6.97×10^{-6}			
	SUM	1.59×10^{-5}	1.33×10^{-5}	9.55×10^{-6}			

where $\bar{\sigma}=(\sigma_{dN}+\sigma_{hN})/2$. The deuteron-nucleon and ^{3}He-nucleon total cross sections are written as σ_{dN} and σ_{hN}, respectively. Here $\rho(\mathbf{b},z)$ is the density distribution of the nucleus at an impact parameter $\mathbf{b}$ and beam-direction coordinate z.

The effective number for configuration $(l_\pi j_n^{-1})J$ is then

$$N_{\rm eff}=\frac{1}{2}\sum_{Lm}\left|S_{JL}\int \exp(i\mathbf{q}\cdot\mathbf{r})D(\mathbf{b})R_\pi(r)R_n(r)Y_{Lm}(\hat{r})d^3r\right|^2 \tag{7}$$

with kinematical factor S_{JL},

$$S_{JL}=\langle l_\pi(l_n\tfrac{1}{2})j_n;J|(l_\pi l_n)L\tfrac{1}{2};J\rangle\left[\frac{2J+1}{2L+1}\right]^{1/2}(-)^{l_n}\left[\frac{(2l_\pi+1)(2l_n+1)}{4\pi(2L+1)}\right]^{1/2}(l_\pi 0 l_n 0|L0)\ , \tag{8}$$

where $R_\pi(r)$ and $R_n(r)$ are the radial wave functions for the pion state and neutron-hole state, respectively. The kinematical factor S_{JL} contains a unitary $9j$ coefficient and a Clebsch-Gordan coefficient with parity conservation.

III. NUMERICAL RESULTS FOR $(d,{}^3\text{He})$ REACTIONS

We calculated the effective numbers $N_{\rm eff}$ for the $(d,{}^3$He) reaction on a ^{208}Pb target at $T_d=600$ MeV for various pionic states with $i_{13/2}$, $f_{5/2}$, $p_{3/2}$, and $p_{1/2}$ neutron-hole states. The results for $N_{\rm eff}$ are summarized in Tables I–IV and the expected spectra are shown in Fig. 4–7. The largest $N_{\rm eff}$ is 1.47×10^{-2} for the $2p$ state with a $p_{3/2}$ neutron hole (Table II) and the corresponding cross section is 65 μb/sr MeV (Fig. 5).

Figures 4 and 5 indicate that the pionic p states are largely populated in the case of $p_{1/2}$ and $p_{3/2}$ neutron holes. The pionic-atom formation cross sections for $j_n=f_{5/2}$ (Fig. 6) are $\frac{1}{3}$ of that of $j_n=p_{3/2}$ (Fig. 5) for all pionic states. The energy spectra for $j_n=f_{5/2}$ shows that the pionic $2p$ and $3d$ states are populated almost equally ($\sim$20 μb/sr MeV) and the resonance peak of the pionic $1s$ state is relatively larger. Figure 7 shows the pionic-atom formation spectrum for $j_n=i_{13/2}$. These cross sections are the smallest among the cases we have considered in this paper.

At $T_d=600$ MeV the momentum transfer is small ($\sim$0.3 fm^{-1}). Therefore, the quasisubstitutional states $[(l_\pi j_n^{-1})J\sim0]$ are preferentially populated. These results indicate that the matching condition $J\sim qR_0$ is also important in the $(d,{}^3$He) reactions as well as in the (n,d) reactions [6].

IV. BACKGROUND ESTIMATION

The feasibility of this reaction for the formation of pionic atoms depends on the background cross section in

TABLE II. The effective numbers N_{eff}, for the $^{208}\mathrm{Pb}(d,{}^3\mathrm{He})$ reaction at $T_d=600$ MeV leading to various pionic states $[(nl)_\pi j_n^{-1}]J$ with $j_n=p_{3/2}$. $S_n=8.264$ MeV. SUM denotes the summed value for each J multiplet with the same pionc and neutron-hole configuration.

l_π	J	$[j_n=p_{3/2}]$					
		1s	2s	3s	4s	5s	6s
0	$\frac{3}{2}$	2.09×10^{-3}	4.07×10^{-4}	1.49×10^{-4}	7.30×10^{-5}	4.06×10^{-5}	2.48×10^{-5}
		2p	3p	4p	5p	6p	
1	$\frac{5}{2}$	3.81×10^{-3}	1.05×10^{-3}	4.45×10^{-4}	2.27×10^{-4}	1.31×10^{-4}	
	$\frac{3}{2}$	4.24×10^{-4}	1.17×10^{-4}	4.94×10^{-5}	2.53×10^{-5}	1.46×10^{-5}	
	$\frac{1}{2}$	1.05×10^{-2}	2.95×10^{-3}	1.26×10^{-3}	6.45×10^{-4}	3.73×10^{-4}	
	SUM	1.47×10^{-2}	4.12×10^{-3}	1.75×10^{-3}	8.98×10^{-4}	5.19×10^{-4}	
		3d	4d	5d	6d		
2	$\frac{7}{2}$	7.08×10^{-4}	3.64×10^{-4}	1.98×10^{-4}	1.16×10^{-4}		
	$\frac{5}{2}$	1.18×10^{-4}	6.06×10^{-5}	3.30×10^{-5}	1.93×10^{-5}		
	$\frac{3}{2}$	3.19×10^{-4}	1.63×10^{-4}	8.84×10^{-5}	5.17×10^{-5}		
	$\frac{1}{2}$	3.19×10^{-4}	1.63×10^{-4}	8.84×10^{-5}	5.17×10^{-5}		
	SUM	1.46×10^{-3}	7.51×10^{-4}	4.07×10^{-4}	2.39×10^{-4}		
		4f	5f	6f			
3	$\frac{9}{2}$	7.20×10^{-6}	5.99×10^{-6}	4.31×10^{-6}			
	$\frac{7}{2}$	1.44×10^{-6}	1.20×10^{-6}	8.62×10^{-7}			
	$\frac{5}{2}$	9.28×10^{-6}	7.74×10^{-6}	5.58×10^{-6}			
	$\frac{3}{2}$	1.39×10^{-5}	1.16×10^{-5}	8.36×10^{-6}			
	SUM	3.18×10^{-5}	2.65×10^{-5}	1.91×10^{-5}			

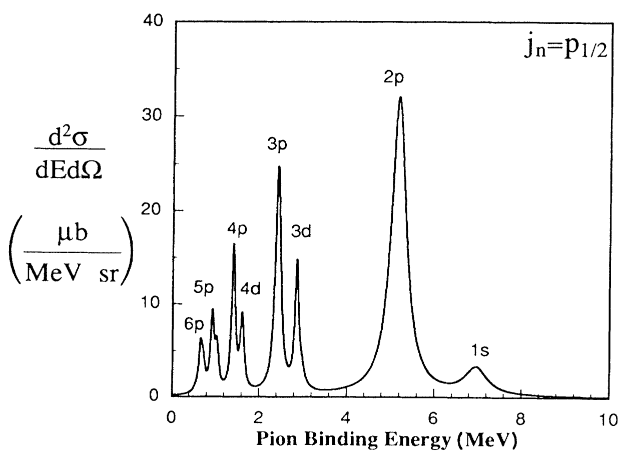

FIG. 4. Expected spectra of the $^{208}\mathrm{Pb}(d,{}^3\mathrm{He})$ reaction at $T_d=600$ MeV leading to various pionic states of configurations $(nl)_\pi j_n^{-1}$ for $j_n=p_{1/2}$. An instrumental resolution of 100 keV FWHM is assumed.

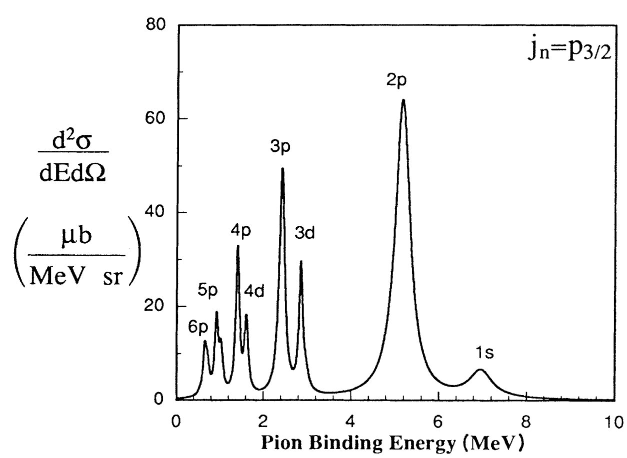

FIG. 5. Expected spectra of the $^{208}\mathrm{Pb}(d,{}^3\mathrm{He})$ reaction at $T_d=600$ MeV leading to various pionic states of configurations $(nl)_\pi j_n^{-1}$ for $j_n=p_{3/2}$. An instrumental resolution of 100 keV FWHM is assumed.

TABLE III. The effective numbers N_{eff}, for the ^{208}Pb(d,^{3}He) reaction at $T_d=600$ MeV leading to various pionic states $[(nl)_\pi j_n^{-1}]J$ with $j_n=f_{5/2}$. $S_n=7.937$ MeV. SUM denotes the summed value for each J multiplet with the same pionic and neutron-hole configuration.

l_π	J	$[j_n=f_{5/2}]$					
		1s	2s	3s	4s	5s	6s
0	$\frac{5}{2}$	2.03×10^{-3}	4.11×10^{-4}	1.52×10^{-4}	7.51×10^{-5}	4.19×10^{-5}	2.57×10^{-5}
		2p	3p	4p	5p	6p	
1	$\frac{7}{2}$	1.10×10^{-3}	3.03×10^{-4}	1.28×10^{-4}	6.54×10^{-5}	3.78×10^{-5}	
	$\frac{5}{2}$	2.14×10^{-4}	5.97×10^{-5}	2.53×10^{-5}	1.30×10^{-5}	7.51×10^{-6}	
	$\frac{3}{2}$	3.00×10^{-3}	8.36×10^{-4}	3.55×10^{-4}	1.82×10^{-4}	1.05×10^{-4}	
	SUM	4.32×10^{-3}	1.20×10^{-3}	5.08×10^{-4}	2.60×10^{-4}	1.50×10^{-4}	
		3d	4d	5d	6d		
2	$\frac{9}{2}$	1.61×10^{-4}	8.44×10^{-5}	4.62×10^{-5}	2.72×10^{-5}		
	$\frac{7}{2}$	5.67×10^{-5}	2.92×10^{-5}	1.59×10^{-5}	9.34×10^{-6}		
	$\frac{5}{2}$	3.40×10^{-4}	1.75×10^{-4}	9.55×10^{-5}	5.60×10^{-5}		
	$\frac{3}{2}$	9.68×10^{-5}	4.97×10^{-5}	2.70×10^{-5}	1.58×10^{-5}		
	$\frac{1}{2}$	3.39×10^{-4}	1.74×10^{-4}	9.44×10^{-5}	5.53×10^{-5}		
	SUM	9.94×10^{-4}	5.13×10^{-4}	2.79×10^{-4}	1.64×10^{-4}		
		4f	5f	6f			
3	$\frac{11}{2}$	6.84×10^{-7}	5.73×10^{-7}	4.13×10^{-7}			
	$\frac{9}{2}$	7.27×10^{-7}	6.06×10^{-7}	4.36×10^{-7}			
	$\frac{7}{2}$	3.20×10^{-6}	2.67×10^{-6}	1.92×10^{-6}			
	$\frac{5}{2}$	4.67×10^{-6}	3.90×10^{-6}	2.81×10^{-6}			
	$\frac{3}{2}$	7.00×10^{-6}	5.85×10^{-6}	4.22×10^{-6}			
	$\frac{1}{2}$	4.12×10^{-5}	3.45×10^{-5}	2.49×10^{-5}			
	SUM	5.75×10^{-5}	4.81×10^{-5}	3.47×10^{-5}			

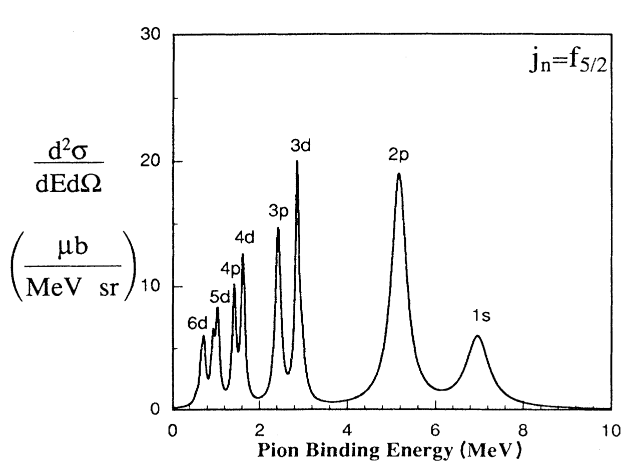

FIG. 6. Expected spectra of the ^{208}Pb(d,^{3}He) reaction at $T_d=600$ MeV leading to various pionic states of configurations $(nl)_\pi j_n^{-1}$ for $j_n=f_{5/2}$. An instrumental resolution of 100 keV FWHM is assumed.

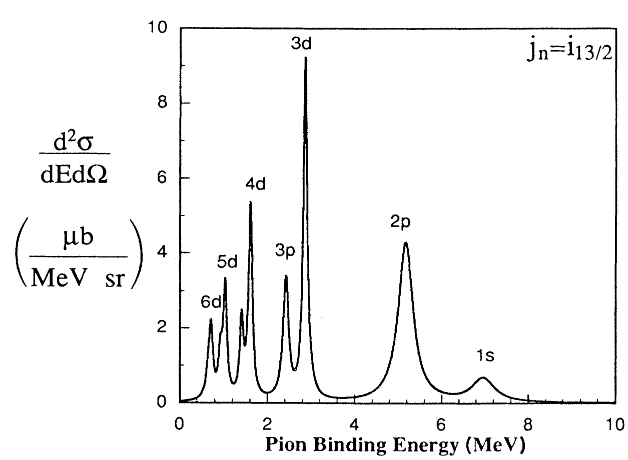

FIG. 7. Expected spectra of the ^{208}Pb(d,^{3}He) reaction at $T_d=600$ MeV leading to various pionic states of configurations $(nl)_\pi j_n^{-1}$ for $j_n=i_{13/2}$. An instrumental resolution of 100 keV FWHM is assumed.

TABLE IV. The effective numbers N_{eff}, for the ^{208}Pb(d,^{3}He) reaction at $T_d=600$ MeV leading to various pionic states $[(nl)_\pi j_n^{-1}]J$ with $j_n=i_{13/2}$. $S_n=9.000$ MeV. SUM denotes the summed value for each J multiplet with the same pionic and neutron-hole configuration.

l_π	J	$[j_n=i_{13/2}]$					
		1s	2s	3s	4s	5s	6s
0	$\frac{13}{2}$	2.25×10^{-4}	4.99×10^{-5}	1.92×10^{-5}	9.59×10^{-6}	5.40×10^{-6}	3.32×10^{-6}
		2p	3p	4p	5p	6p	
1	$\frac{15}{2}$	3.15×10^{-5}	1.02×10^{-5}	4.55×10^{-6}	2.39×10^{-6}	1.41×10^{-6}	
	$\frac{13}{2}$	3.03×10^{-7}	9.78×10^{-8}	4.38×10^{-8}	2.30×10^{-8}	1.35×10^{-8}	
	$\frac{11}{2}$	9.52×10^{-4}	2.64×10^{-4}	1.12×10^{-4}	5.72×10^{-5}	3.31×10^{-5}	
	SUM	9.83×10^{-4}	2.74×10^{-4}	1.16×10^{-4}	5.97×10^{-5}	3.45×10^{-5}	
		3d	4d	5d	6d		
2	$\frac{17}{2}$	4.39×10^{-8}	1.47×10^{-8}	6.71×10^{-9}	3.64×10^{-9}		
	$\frac{15}{2}$	7.51×10^{-10}	2.51×10^{-10}	1.15×10^{-10}	6.22×10^{-11}		
	$\frac{13}{2}$	3.69×10^{-5}	1.95×10^{-5}	1.07×10^{-5}	6.32×10^{-6}		
	$\frac{11}{2}$	1.26×10^{-6}	6.63×10^{-7}	3.65×10^{-7}	2.15×10^{-7}		
	$\frac{9}{2}$	4.61×10^{-4}	2.40×10^{-4}	1.32×10^{-4}	7.74×10^{-5}		
	SUM	4.99×10^{-4}	2.61×10^{-4}	1.43×10^{-4}	8.39×10^{-5}		
		4f	5f	6f			
3	$\frac{19}{2}$	5.26×10^{-8}	4.35×10^{-8}	3.11×10^{-8}			
	$\frac{17}{2}$	1.21×10^{-9}	1.00×10^{-9}	7.18×10^{-10}			
	$\frac{15}{2}$	4.84×10^{-8}	4.16×10^{-8}	3.05×10^{-8}			
	$\frac{13}{2}$	2.93×10^{-9}	2.52×10^{-9}	1.85×10^{-9}			
	$\frac{11}{2}$	2.88×10^{-6}	2.40×10^{-6}	1.73×10^{-6}			
	$\frac{9}{2}$	2.00×10^{-7}	1.67×10^{-7}	1.20×10^{-7}			
	$\frac{7}{2}$	1.89×10^{-5}	1.57×10^{-5}	1.13×10^{-5}			
	SUM	2.21×10^{-5}	1.84×10^{-5}	1.32×10^{-5}			

the range of 140 MeV excitation. No experimental data are available at such high excitation for neither (d,^{3}He) nor (d,t) cross sections. Recently, the (n,d) spectrum on ^{208}Pb in the range of 140 MeV excitation was measured at the TRIUMF CHARGEX facility [7]. The spectrum shows a distinct quasifree π^- production component above 140 MeV and a flat background of about 0.4 mb/sr MeV. We assume a qualitatively same spectrum for the (d,^{3}He) reaction and evaluate the flat background for the (d,^{3}He) reaction to be 40 μb/sr MeV from the (n,d) data by simply assuming a reduction factor $\frac{1}{10}$ for (d,^{3}He).

An overall spectrum at $T_d=600$ MeV including the four neutron holes is shown in Fig. 8 with flat background cross sections of 40 μb/sr MeV. The substitutional states make the largest peaks and the dominant contributions come from the 2p pionic state with neutron $p_{3/2}$ and $p_{1/2}$ hole states. We can also see the pionic 1s state formation at $Q\sim-134$ MeV as a shoulder in Fig. 8. This figure shows that the pionic-atom formation cross sections are much larger than the flat-background cross

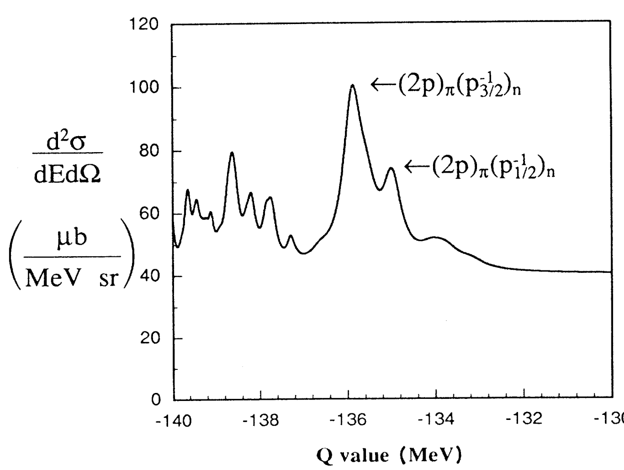

FIG. 8. Expected spectra of the ^{208}Pb(d,^{3}He) reaction at $T_d=600$ MeV, where all the neutron holes ($p_{1/2}$,$p_{3/2}$,$f_{5/2}$,$i_{13/2}$) are taken into account. An instrumental resolution of 100 keV FWHM and a flat background of 40 μb/sr MeV are assumed.

sections.

Then, we estimate the quasifree (unbound) π^- production cross section just above the π^- production threshold in the $(d,{}^3\mathrm{He}\ \pi^-)$ reaction in order to study the ^{3}He spectrum near the threshold. The nucleon inside the target nucleus moves with momentum p and energy $E=\sqrt{M^2+p^2}$ where we neglect the binding energy for the nucleon. We assume also that $(A-1)$ nucleons are spectators. The outgoing pion momentum $\mathbf{k}_\pi$ and energy E_π from the $(d,{}^3\mathrm{He})$ reactions are written as

$$\mathbf{q}=\mathbf{p}_d-\mathbf{p}_h=\mathbf{k}_\pi-\mathbf{p}\ ,$$
$$\omega=E_d-E_h=E_\pi-E\ . \tag{9}$$

The effective number formalism may be written as [15]

$$\frac{d\sigma}{d\Omega_d dE_d}=\left[\frac{d\sigma}{d\Omega}\right]^{\mathrm{lab}}_{dn\to{}^3\mathrm{He}\,\pi} R(\omega,\mathbf{q})\ . \tag{10}$$

The response function $R(\omega,\mathbf{q})$ is written as

$$R(\omega,\mathbf{q})=N_{\mathrm{eff}}\int d^3p\,\rho_p(\mathbf{p})\delta(\omega-E_\pi+E)\ , \tag{11}$$

where

$$N_{\mathrm{eff}}=\int d^3r\,\rho(\mathbf{r})\exp\left[-\int_{-\infty}^{\infty}\sigma\rho(\mathbf{b},z')dz'\right]\ . \tag{12}$$

Here $\rho_p(\mathbf{p})$ is the momentum distribution and $\rho(\mathbf{r})$ is the neutron distribution in the target nucleus and they are normalized to 1 and to the neutron number, respectively. For simplicity, we take $\rho_p(\mathbf{p})=N\exp(-p^2/p_0^2)$ with $p_0=177$ MeV/c and $\rho(\mathbf{r})=\rho_0/\{1+\exp[(r-R)/a]\}$. We determined p_0 so as to reproduce the same $\langle p^2\rangle$ as Fermi distribution with $p_F=280$ MeV/c.

The results are shown in Fig. 9 with the pionic-atom formation spectrum. We assume 40 μb/sr MeV to be the flat background cross section as in Fig. 8. The spectrum shows that the resonant peaks of pionic atom formation are significantly higher than the quasifree π^- formation spectrum.

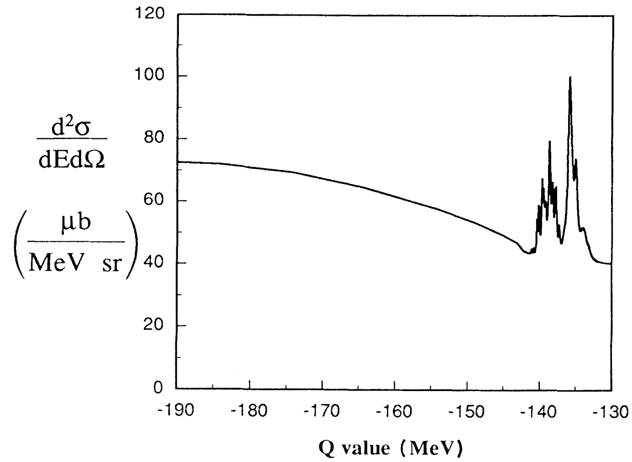

FIG. 9. Expected spectra for the ^{208}Pb$(d,{}^3\mathrm{He})$ reaction leading to various pionic atom states for all the neutron holes and an expected spectrum leading to quasifree unbound pionic states at $T_d=600$ MeV. An instrumental resolution of 100 keV FWHM and a flat background of 40 μb/sr MeV are assumed.

V. SUMMARY

We have studied theoretically the possible use of the $(d,{}^3\mathrm{He})$ reaction for the formation of deeply bound pionic states. The calculation was made at 600 MeV because the cross section is considered to be the largest due to the largest elementary cross section and small momentum transfer. We find the preferential population of quasisubstitutional states $[(nl)_\pi j_n^{-1}]J=0$ as in the case of the (n,d) reaction. The pionic $2p$ state with neutron holes $3p_{1/2}$ and $3p_{3/2}$ are preferentially populated for a ^{208}Pb target. It was found that the main structure of the spectrum showed up well above the assumed background.

It is extremely interesting to examine the fine structure of $[(nl)_\pi j_n^{-1}]J$ multiplets experimentally by using the $(d,{}^3\mathrm{He})$ reaction, where the fine structure is caused by the pion-neutron residual interaction. As has been discussed for the case of (n,d) reactions [6], each member of the multiplet has different incident-energy dependence. Hence, one can, in principle, discriminate the multiplet members. The $(d,{}^3\mathrm{He})$ reaction is more suited for this purpose than the (n,d) reaction because of a good energy resolution and a high beam intensity. Such resolved multiplets, if observed, would give important information on the pion-neutron-hole interaction.

We require very high-resolution spectroscopy because we expect many discrete peaks of small natural widths. To this, Yamazaki *et al.* [8] have recently studied the possible use of the inverse kinematics where heavy nuclei are injected on light target nuclei and the recoiled light ejectiles are detected after producing pionic atoms in heavy nuclei. If coupled with a high-quality heavy ion beam as produced by SIS/ESR of GSI, one may get an energy resolution as good as 100 keV.

ACKNOWLEDGMENTS

We would like to thank I. Tanihata and D. Hirata for useful comments. This work was performed under the auspices of Special Researcher's Basic Science Program of RIKEN.

[1] H. Toki and T. Yamazaki, Phys. Lett. B **213**, 129 (1988).
[2] H. Toki, S. Hirenzaki, T. Yamazaki, and R. S. Hayano, Nucl. Phys. **A501**, 653 (1989).
[3] M. Iwasaki, A. Trudel, A. Celler, O. Häusser, R. S. Hayano, R. Helmer, R. Henderson, S. Hirenzaki, K. P. Jackson, Y. Kuno, N. Matsuoka, J. Mildenberger, C. A. Miller, H. Outa, H. Sakai, H. Toki, M. Vetterli, Y. Watanabe, T. Yamazaki, and S. Yen, Phys. Rev. C **43**, 1099 (1991).
[4] T. Yamazaki *et al.*, SATURNE proposal No. 214 (1988); R. S. Hayano and T. Miyamoto, private communication.

[5] J. Nieves and E. Oset, Nucl. Phys. **A518**, 617 (1990).
[6] H. Toki, S. Hirenzaki, and T. Yamazaki, Nucl. Phys. **A530**, 679 (1991).
[7] A. Trudel, private communication.
[8] T. Yamazaki, R. S. Hayano, and H. Toki, Nucl. Instrum. Methods **A305**, 406 (1991).
[9] C. Dover, L. Ludeking, and G. Walker, Phys. Rev. C **22**, 2073 (1980).
[10] H. W. Fearing, Phys. Rev. C **16**, 313 (1977).
[11] C. Richard-Serre, W. Hirt, D. F. Measday, E. G. Michaelis, M. J. M. Saltmarsh, and P. Skarek, Nucl. Phys. **B20**, 413 (1970).
[12] D. Aebischer, B. Favier, L. G. Greeniaus, R. Hess, A. Junod, C. Lechanoine, J.-C. Nikles, D. Rapin, and D. W. Werren, Nucl. Phys. **B106**, 214 (1976).
[13] J. Hoftiezer, Ch. Weddigen, B. Favier, S. Jaccard, P. Walden, P. Chatelain, F. Foroughi, C. Nussbaum, and J. Piffaretti, Phys. Lett. **100B**, 462 (1981).
[14] E. Aslanides, R. Bertini, C. Bing, F. Brochard, Ph. Gorodetzky, F. Hibou, T. S. Bauer, R. Beurtey, A. Boudard, G. Bruge, H. Catz, A. Chaumeaux, P. Couvert, H. H. Duhm, D. Garreta, G. Igo, J. C. Lugol, M. Motoba, Y. Terrien, L. Bimbot, Y. LeBornec, and B. Tatischeff, Phys. Rev. Lett. **39**, 1654 (1977).
[15] G. F. Bertsch and O. Scholten, Phys. Rev. C **25**, 804 (1982).